JOURNAL OF MAGNETIC RESONANCE **126,** 9–17 (1997)
ARTICLE NO. MN971149

Mutual Inductance in the Bird-Cage Resonator*

James Tropp

General Electric Medical Systems, 47697 Westinghouse Drive, Fremont, California 94539

Received July 2, 1996; revised February 21, 1997

Formulas are derived to account for the effect of the mutual inductances, between all meshes, upon the electrical resonance spectra bird-cage resonators, and similar structures such as the TEM resonator of P. K. H. Röschmann (United States Patent 4,746,866) and J. T. Vaughan *et al.* **(***Magn. Reson. Med.* **32, 206, 1994). The equations are parameterized in terms of isolated mesh frequencies and coupling coefficients, and ought therefore apply not only to simple magnetic couplings used in the derivation, but to electromagnetic couplings as well. A method for measuring the coupling coefficients—applicable to shielded as well as unshielded resonators—is described, based upon the splitting of frequencies in pairs of coupled resonators; and detailed comparisons are given between calculated and measured resonance spectra: for bird-cage resonators, with and without shields, and for the TEM resonator.**

INTRODUCTION

Despite widespread use of the bird-cage resonator (*1*) and the appearance of several works aimed at elucidating its circuit theory, the effects of mutual inductance upon its electrical resonance spectrum have not yet been fully explained. Joseph and Lu (*2*) gave a Toeplitz matrix for the mutual inductance of the rungs of the high-pass bird cage, but ignored the end rings; Tropp (*3, 4*) showed that couplings between near-neighbor meshes dominate the low-pass resonator, but neglected remote neighbors; Harpen (*5*) solved the ingenious but perhaps unrealistic model of an infinitely long bird cage comprising an infinity of closely spaced axial segments; Pascone *et al.* (*6*) painstakingly calculated the mutual inductances between all pairs of conductors in a conventional bird cage, but cast their final results in transmission-line theory, which, despite its grace and concision, tends somewhat to submerge rather than display the effects of the couplings.

We now present an improved theory of mutual inductance in the bird-cage resonator, based upon the exact solution of a circuit model which is both realistic and fairly complete. Formulas for the positions of electrical resonances are given in terms of simple, measurable circuit quantities—resonant frequencies of single meshes, and coefficients of coupling between them—which comprise a complete set of design parameters for construction or computer simulation. Furthermore, the effects of near and remote couplings are separated, so that the theory may be implemented in varying degrees of approximation. The theory predicts the spectrum of resonant frequencies to a mean accuracy of 0.5% or better for a bird cage in free space—a condition that is often well approximated in practice. An empirical method for dealing with the case of a bird-cage resonator inside a close-fitting electromagnetic shield is also discussed briefly.

We assume that the reader is acquainted with the ladder structure of the bird-cage resonator (as illustrated in Fig. 1), and that the terms ''rungs'' and ''end rings'' are familiar. All bird cages of N meshes will be assumed to have N-fold rotational symmetry about a cylinder axis. The theoretical development is followed by experimental results. The theory is given first for the low-pass resonator and then modified for the high-pass. We then treat an elegant and efficient volume resonator—introduced by Röschmann (*7*) and further developed by Vaughan *et al.* (*8*)—which, although neither low- nor high-pass, is still of the bird-cage type, inasmuch as it comprises a cylindrical array of identical coupled resonators. Since this resonator is derived from a type of coaxial waveguide structure which supports transverse electromagnetic fields, it has been dubbed the TEM resonator; it is also closely related to the ''free-element'' resonator of Wen *et al.* (*9*).

THEORY

Circuit models, nomenclature, and equations. The present theory is patterned on our earlier treatment of the low-pass resonator (*3*), in which circuit equations were solved for the mesh currents, I_n, of the lumped-element LC ladder network shown in Fig. 2A. We will take for granted the applicability of the lumped-element model—even as the circuit dimensions approach the wavelength of the operating frequency—since similar models are widely

* Preliminary accounts of this work were presented at meetings of the Society of Magnetic Resonance in Medicine, in 1992 and 1993.

1090-7807/97 $25.00

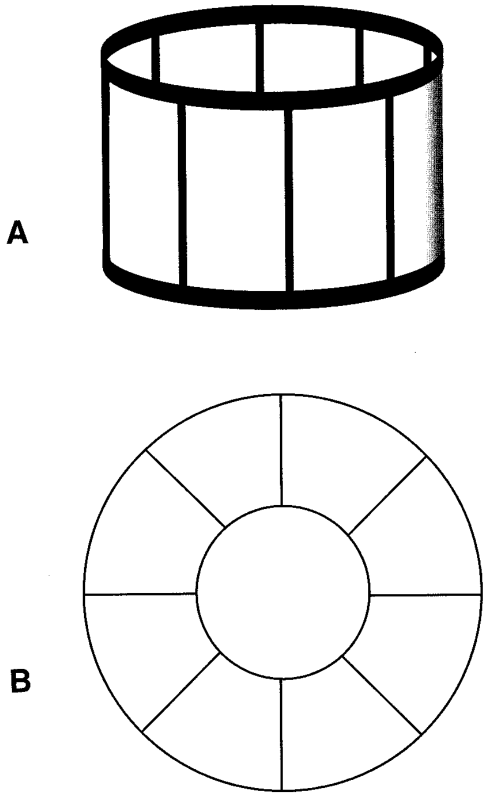

FIG. 1. The geometry (A) and topology (B) of a bird-cage resonator. The meaning of such terms as ''ladder network,'' ''rungs,'' and ''end rings'' should be self-evident. The example given is a bird cage of eight rungs, commonly known (by a slight abuse of language) as a bird cage of eight meshes or eight elements.

used in microwave theory to represent the equivalent circuits of distributed components, such as stripline sections or cavity resonators (*10*).

Still, the interpretation of model circuit parameters is not free of ambiguity. For example, the quantity M in Fig. 2A provides an inductive coupling term (i.e., linear in frequency and bilinear in current) between adjacent meshes in the circuit equations. This is true whether we regard it as physically representing the *self*-inductance of the ladder rung, or the *mutual* inductance between two meshes, or a combination of the two. In fact, the present work will retain the unadorned symbol M exclusively for the shunt self-inductance, and will reserve its subscripted counterpart, M_{ij}, for the mutual inductance between meshes. In any case, our objective is to write the circuit equations directly in terms of measurable quantities (resonant frequencies and coupling coefficients) and the pictorial circuit model is best thought of as an aid to that end, rather than as a representation of reality in itself.

We have found it expeditious to derive the circuit equations from energy functions, using the Lagrangian formulation. This method—in addition to being nearly foolproof, and providing a clear inventory of the requisite dynamical variables—was also employed by Brillouin in his classic study of periodic ladder circuits (*11*), which so closely prefigures the development of the bird-cage. To recap briefly, the circuit is described by a suitable set of charges and their time derivatives (currents), in exact analogy to the positions and velocities of particles in mechanics. Pursuing the analogy, the circuit energy is partitioned into magnetic (or ''kinetic'') and electric (or ''potential'') energies, which we denote by T and V, respectively—borrowing (as has been customary in the electrical literature) the nomenclature of mechanics (*12*). The circuit equations are then obtained by differentiation,

$$\frac{d}{dt}\left(\frac{\partial T}{\partial I_n}\right) + \frac{\partial V}{\partial q_n} = 0, \qquad [1]$$

where $I_n = dq_n/dt$ is the current associated with displacement of the nth charge. In the case of the bird cage, since we may assume that all currents are harmonic, it is convenient, after

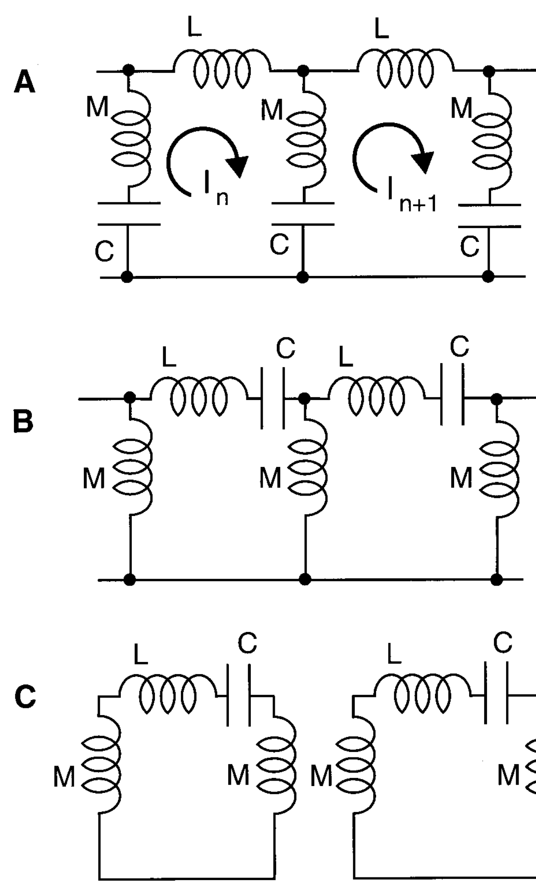

FIG. 2. Circuit models for bird-cage resonators: (A) low pass, (B) high pass, and (C) TEM resonator. Refer to the text for further details.

the differentiations, to perform Laplace transformation, and write the nth current as I_n and the nth charge as I_n/s, where $s = i\omega$ is the complex frequency. In fact, we will slightly reorder this practice in the sequel, by writing V directly as a function of I_n/s, prior to the differentiations, for the purposes of which I_n and I_n/s must then be treated as separate independent variables.

Within the context of the Lagrangian formalism, it is worthwhile discussing (even belaboring) some particulars concerning the choice of mesh currents as dynamical variables. In the terminology of formal circuit theory (*13*), a diagram of the type in Fig. 1B represents a planar, unhinged graph, with $3N$ branches and $2N$ nodes, which is therefore described by N mesh currents, if we neglect the so-called "outer mesh." Considering the bird cage as a reentrant transmission line, neglect of the outer mesh is tantamount to considering only balanced transmission modes, and ignoring the (unbalanced) corotating end-ring mode. Since the end-ring modes are of no practical importance, the N mesh currents provide a complete basis for our analysis. One important consequence is that the most general form of the (circuit theoretic) magnetic energy is then a bilinear function of the mesh currents; this means that the mutual inductances between open-circuit segments of the bird cage (as opposed to theose between closed-circuit meshes) are not a *sine qua non* of the theory.

The low-pass resonator. We start with the circuit model of Fig. 2A [see also Ref. (*3*)] for which the magnetic energy is written in terms of the mesh currents I_n as

$$T = \sum [(L/2)I_n^2 + (M/2)(I_n - I_{n+1})^2]. \qquad [2]$$

Here L is the contribution of the end rings to the self-inductance of a single isolated mesh of the coil; M is the self-inductance of the rung of the bird-cage ladder; and the sum is over all meshes.

To account for mutual inductance (*14*), we add to a term comprising the energy due to flux coupling between all meshes,

$$T_{\text{flux}} = \sum (M_{nk}/2)I_nI_k, \qquad [3]$$

where the M_{nk} are mutual inductances between meshes, and the sum runs over all pairs of meshes with $n \neq k$. We separate the self-inductance of a leg from the mutual inductance between adjacent meshes, even though both produce similar coupling terms in the circuit equations. Combining [2] and [3] gives the complete magnetic energy (which is bilinear in mesh currents, as noted above); the requisite term for electric energy is $V = (1/2s^2C)\,\Sigma\,[I_{n+1} - I_n]^2$, where s is the complex angular frequency $i\omega$. Then, assuming N-fold rotational symmetry about the bird-cage axis and treating I_n/s as independent variables in V, we perform the differentiations indicated in [1] to obtain the Kirchoff voltage equations (*11, 14*):

$$s[(L + 2M) + 2/sC]I_n - [sM + 1/sC][I_{n+1} + I_{n-1}] + s\{M_{n,n+N/2}I_{n+N/2} + \sum_{k=1}^{N/2-1} M_{n,n+k}[I_{n+k} + I_{n-k}]\} = 0. \qquad [4]$$

There are N such equations (indexed by n) all identical, due to symmetry; the sum over k makes use of the Toeplitz property of the bird cage: that mutual inductance between two meshes depends only upon the difference in their indices.

Equation [4] can be written (dividing by $L + 2M$, and multiplying by s) to replace the circuit components by frequencies and coupling coefficients:

$$[s^2 + 2\omega_a^2]I_n - \omega_a^2[I_{n+1} + I_{n-1}] + s^2\{\xi_{n,n+N/2}I_{n+N/2} + \sum_{k=1}^{N/2-1} \xi_{n,n+k}[I_{n+k} + I_{n-k}]\} = 0, \qquad [5]$$

where $\sqrt{2}\omega_a$ is the resonant frequency of an isolated mesh of the bird cage, and the ξ are coupling coefficients given by $\xi_{n,n+1} = (M_{n,n+1} - M)/(L + 2M)$, and $\xi_{n,n+k} = (M_{n,n+k})/(L + 2M)$, for $k \geqslant 2$. The Toeplitz property again dictates that these coefficients depend only upon the "difference" index, k, so that we may, without losing generality, set $n = 1$ in the sequel. The virtue of [5] lies in the replacement of model circuit components—whose significance is not always without ambiguity—with phenomenological parameters (frequencies and coupling coefficients) whose measurement is easily prescribed and whose meaning is therefore clear. The nearest-neighbor coefficient, $\xi_{n,n+1}$, is unique in that it embodies both flux coupling and a term derived from the fact that adjacent meshes have a shared conductive path. It is equivalent, except for a sign change, to the coefficient $(\omega_a/\omega_b)^2$ of Ref. (*3*), although that earlier work mentions flux coupling only in passing.

Equation [5] is solved, on the assumption of traveling-wave eigenfunctions (*3, 11*), to yield the following expression for the Jth eigenvalue,

$$\omega_J^2 = \frac{2\omega_a^2[1 - \cos(2\pi J/N)]}{1 + S_J}, \qquad [6]$$

where we define

$$S_J = \xi_{1,N/2+1}\cos(\pi J) + 2\sum_{k=1}^{N/2-1} \xi_{1,1+k}\cos[2\pi Jk/N]. \qquad [7]$$

The high-pass resonator. We turn to the circuit model of Fig. 2B. While the magnetic energy functions are the same here as for the low-pass resonator, the electric energy function differs:

$$V = \frac{1}{2s^2C} \sum I_n^2. \quad [8]$$

The Kirchoff equations are

$$s[(L + 2M) + 1/sC]I_n - sM[I_{n,n+1} + I_{n,n-1}] + s\{M_{n,n+N/2}I_{n+N/2} + \sum_{k=1}^{N/2-1} M_{n,n+k}[I_{n+k} + I_{n-k}]\} = 0, \quad [9]$$

leading to the following expression for the eigenvalues,

$$\omega_J^2 = \frac{\omega_a^2}{1 + S_J}, \quad [10]$$

where ω_a is now the isolated single-mesh frequency, and the other symbols have the meanings given earlier; in particular, the definition of the various coupling coefficients is exactly as that for the low-pass resonator, since the magnetic energy is identical in both low- and high-pass cases.

The TEM resonator. Röschmann has analyzed the TEM resonator by considering the characteristic mode impedances of multiconductor cavities (*15*); we arrive at similar results by means of a simpler treatment, based upon the circuit model of Fig. 2C. Since the TEM resonator is essentially a collection of identical resonator elements, symmetrically arrayed inside a conducting cylinder (which we may take as an electrical ground), the natural circuit parameters are therefore the resonant frequency of an isolated resonant element, and the coefficients of coupling between neighboring elements. But these are just the parameters chosen above for our bird-cage equations. The cylindrical symmetry of the TEM resonator also suggests that its eigenfunctions, like those of the ordinary bird cage, should be found by imposing a period boundary condition. The resulting theory is very close to that which has been given for the free-element resonator (*9*).

The electric-energy function for our circuit model is the same as that of the high-pass resonator, while the magnetic energy is given by

$$T = \sum \frac{1}{2}(L + 2M)I_n^2 + \sum (M_{nk}/2)I_nI_k. \quad [11]$$

While it is not immediately apparent from the form of [11], a derivation along the lines leading to [6] and [10] yields an expression for the eigenvalues identical in form to Eq. [10] for the high-pass resonator; note, however, that the definition of nearest-neighbor coupling is now $\xi_{n,n+1} = (M_{n,n+1})/(L + 2M)$. Furthermore, the signs of the coupling coefficients are reversed from those of the conventional bird cage (as discussed later) which leads to a reordering of the resonant spectrum. The mode consisting of equal mesh currents in the same direction (corresponding to the end-ring mode of the high-pass bird cage) is now the lowest frequency mode in the spectrum; it is called the cyclotron mode (*8*), since it produces a B field directed along the azimuth. The next mode up is the useful, or principal, mode, and the others follow in the same ascending order as observed for the *low*-pass bird cage.

The coefficients of coupling. We have introduced coupling coefficients to describe the magnetic interaction between pairs of circuit meshes; by combining and collating the (bilinear) cross terms of Eq. [2] with their corresponding terms in Eq. [3], one easily shows that each pair of meshes contributes a separate term to the overall magnetic energy. The couplings may therefore be determined by isolating (or, so to speak, excising) each pair of meshes, in turn, from the rest of the bird-cage structure. For each pair, we construct a model circuit of two meshes which suitably mimics the required geometry, and determine the coupling from measurements of the mode frequencies. Since the signs of the coupling coefficients are essential, and depend in nonobvious ways upon the circuit geometry, we give a detailed discussion. Figure 3 shows some representative geometries, which, despite their differences, may all be described by the same generic matrix for the Kirchoff voltage equations, which for two meshes labeled with indices m and n has the form

$$\mathbf{K} = \begin{bmatrix} s^2 + \omega_0^2 & s^2\xi_{nm} \\ s^2\xi_{nm} & s^2 + \omega_0^2 \end{bmatrix}. \quad [12]$$

Assuming that the two meshes are geometrically and electrically identical, the solution of [12] gives two normal modes, designated as symmetric and antisymmetric, corresponding to co- and counterrotating mesh currents. The mode frequencies are

$$\omega_\pm = \omega_0/\sqrt{1 \pm \xi}, \quad [13]$$

where the plus and minus subscripts denote symmetric and antisymmetric modes, and ω_0 is the resonant frequency of a single mesh in isolation.

Since Fig. 3A may be taken to represent a pair of near-neighbor meshes, its coefficient is given by $\xi_{n,n+1} = (M_{n,n+1} - M)/(L + 2M)$, while the expression for Figs. 3B and 3C would be $\xi_{nm} = M_{nm}/(L + 2M)$. Nonetheless, in practice,

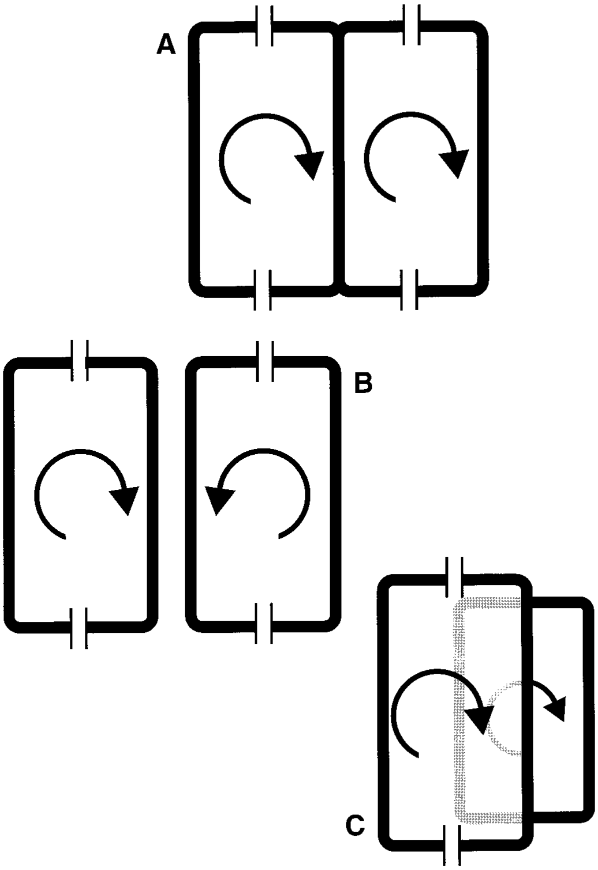

FIG. 3. Model circuits for the determination of coupling constants: (A) nearest neighbor for the conventional bird cage (high or low pass), (B) remote neighbor for the conventional bird cage, and (C) near or remote neighbor for the TEM resonator.

the only phenomenological difference between the circuit of Fig. 3A and those of Figs. 3B and 3C is that the former is strongly coupled, while the latter are weakly coupled. We have shown Fig. 3A in a high-pass configuration, for which the analysis of Eqs. [12] and [13] applies; the low-pass case can be explicitly analyzed (*4*), but the algebra is much more cumbersome, and the end results are in any case equivalent, since the high- and low-pass resonators have the same magnetic energy. We therefore recommend the high-pass configuration for the determination of magnetic interactions. While the solution [13] holds for all coupling regimes, with the proviso that the two meshes, when isolated from each other, are identically tuned, this requirement can be relaxed in the weak-coupling regime, and a perturbation expression used to account for a mistuning error,

$$(\omega_+ - \omega_-)^2 \approx \delta^2 + (\xi\omega_0)^2, \qquad [14]$$

where δ is the mistuning error (in megahertz) of two meshes when uncoupled from each other. Expression [14] simplifies the measurement procedure for weakly coupled meshes, since it is easier to apply the correction for (slightly) mistuned circuit pairs than to trim them into exact (or near exact) coincidence. However, for strongly coupled meshes, the measurements require the extra labor of trimming the two uncoupled meshes, as nearly as possible, to exact coincidence. Operational details are given under Experimental Procedures.

Despite the apparent simplicity of the notion of symmetric and antisymmetric modes, what is actually meant depends in detail upon how one specifies the sign, or sense, of a mesh current. This is trivial for coplanar loops, where the notions of clockwise (positive) and counterclockwise (negative) circulation always suffice. But for current loops mounted on an orientable surface, such as the outside of a circular cylinder, it is required to give the sign of the current in terms of the normal vector derived (by the right-hand rule) from its sense of circulation. For the conventional bird cage, the current paths are confined to the surface of the cylinder, and the normal vectors will have two possible directions: radially inward, or outward. A positive current will be taken to have an *inward*-directed normal (when viewed from outside the cylinder this is consistent with choosing a clockwise current positive in the planar case), and two circulating currents will be considered to have the same sign if their normals have the same sense. This leads to the seeming paradox that two currents of the same sign will nonetheless circulate in opposite directions—as reckoned in rectilinear coordinates—when they are spaced apart by an azimuth of π on the cylinder surface. The correctness of this result may be verified by a tedious calculation of the magnetic flux for the useful mode of the bird-cage resonator.

With the above considerations (which apply equally to the high- and low-pass resonators), it is seen that the mutual inductance (and also the coupling coefficient) for any pair of meshes in a conventional bird cage is negative: that is, their symmetric mode of resonance (assuming them to be excised from the rest of the bird cage) will always be higher in frequency. This may be demonstrated by considering the magnetic energy, or by simple experiment.

Similar principles apply to the TEM resonator, with modifications to accommodate its geometry. Here the current loops lie in diametral planes, so their normals point in the direction of the azimuth θ. Assuming a right-handed cylindrical system, a positive mesh current will be taken as one whose normal (determined by the right-hand rule) points in the positive θ direction. It is then seen that the mutual inductance and the sign of the coupling coefficients are in all cases positive, even though two positive currents separated by an azimuth of π will be oppositely directed as reckoned

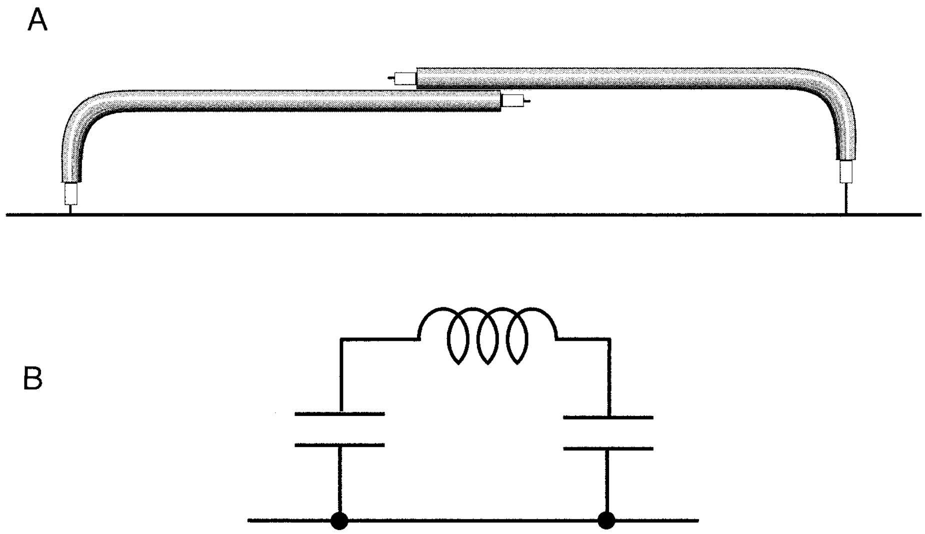

FIG. 4. (A) The ''grab-bar'' resonant element of the TEM resonator, as described in detail under Experimental Procedures, along with (B) its equivalent circuit.

in Cartesian coordinates. This echoes the behavior for the conventional bird cage.

The shielded bird-cage. Sometimes a bird-cage resonator is operated inside a conductive shield, to minimize interactions with its surroundings. Inasmuch as the shield has perfect cylindrical symmetry, it cannot perturb the symmetry of the circuit equations: therefore, the forms of expressions [4] and [9] cannot be altered, although the parameters must change. Under quasistatic conditions the main effect of the shield is to alter self- and mutual inductances of the various meshes; but even beyond this limit, the shifts in mesh frequencies and coupling coefficients should suffice for calculation of the mode resonance positions. Since suitable calculation tools for the theoretical evaluation of these shifts are not widely available, and since the labor in retuning a shielded resonator may be considerable, we judged it desirable to attempt measurements of resonant frequencies and coupling coefficients inside a conductive shield, to test the accuracy of predictions made on the basis of the first- and second-neighbor interactions. The procedures and results are given below.

EXPERIMENTAL PROCEDURES

Construction of resonators. Experiments in free space were performed on low-pass resonators of 16 and 8 meshes, on a high-pass resonator of 8 meshes, and on a TEM resonator of 8 elements. The 16-mesh resonator was of copper tape and porcelain chip capacitors (American Technical Ceramics, Dielectric Labs Inc.) on a 9.75 in. o.d. fiberglass cylinder. The width of the ladder rungs was nominally 0.375 in.; that of the end ring was 0.75 in.; 100 pF capacitors were used; and the window aperture was 6.50 $\times$ 1.54 in. High- and low-pass resonators of 8 meshes were fabricated on flexible circuit board substrates (RT Duroid, Rogers Corp.) mounted on 10.76 in. o.d. fiberglass cylinders. The width of the rungs was 0.5 in., and that of the end ring was 1.0 in.; the window aperture was 3.72 $\times$ 6.50 in. Capacitor values were 390 pF for the high pass and 100 pF for the low pass.

Low-pass resonators of 16 and 8 meshes for shielding experiments were similar to those above, except both had an o.d. of 10.4 in. The RF shield was formed of Mylar-backed copper sheet soldered inside a fiberglass cylinder of length 14.8 in. and i.d. 12.4 in., which was fitted with a centering ring at one end to ensure axial and radial centering of the resonator inside the shield.

The TEM resonator was build on an acrylic cylinder of o.d. 7.4 in. and height 10.7 in., with a ground plane of Mylar-backed copper, soldered to form a continuous skin on the outside. The individual resonant elements were formed of two 5.5 in. lengths of 0.141 in. semirigid coaxial cable, whose shields were overlapped by 0.25 in. and soldered together, forming a structure 10.7 in. long, with a continuous outer, and discontinuous inner, conductor. The two remote ends of the cables were bent to form a structure resembling a grab bar (Fig. 4), with a standoff of 0.8 in. The ends were then trimmed to expose about 0.2 in. of the dielectric, and 0.1 in. of the center pin.

For mounting these elements, eight through holes (0.151 diam) were drilled on each of two axially aligned bolt circles, located 1 in. in from either end of the acrylic cylinder. Each grab-bar element was then mounted inside the cylinder, to span the distance between the bolt circles, with its shaft parallel to the axis, and its standoff directed

TABLE 1

Comparison of Calculated and Observed Resonant Frequencies (in MHz) of Various Bird-Cage Resonators, Together with Observed Coupling Coefficients and Isolated Mesh Frequencies Used in the Calculations[a]

16-mesh low-pass bird cage	46.00 MHz[b]							
Observed	19.83	32.12	39.56	44.78	48.05	50.43	51.51	52.49
Calculated	19.96	32.22	39.87	44.88	48.24	50.38	51.57	52.49
Coupling	−0.305	−0.0296	−0.0116	−0.0067	−0.0044	−0.0041	−0.0031	−0.0035
8-mesh low-pass bird cage	39.78 MHz[b]							
Observed	26.21	39.02	44.66	46.23				
Calculated[c]	26.02	39.13	44.93	46.07				
8-mesh high-pass bird cage	19.86 MHz[b]							
Observed	24.16	19.45	17.20	16.31				
Calculated	24.01	19.54	17.17	16.26				
Coupling	−0.252	−0.022	−0.021	−0.011				
8-element TEM resonator	147.2 MHz[b]							
Observed	137.24	143.56	149.22	152.56	154.17			
Calculated	136.42	142.70	149.66	152.15	155.04			
Coupling	0.0555	0.0164	0.0102					

[a] Calculated and observed frequencies are tabulated by mode number, starting from principle mode; coupling coefficients are tabulated in the order first neighbor, second neighbor, etc.

[b] Isolated single-mesh frequency.

[c] Couplings are the same as those for 8-mesh high pass, below.

radially inward. The center pins just protruded through the holes in the cylinder, and so could be bent over and soldered to the copper ground skin outside. So installed, each element was then equivalent to a low-pass pi circuit (Fig. 4), whose frequency could be trimmed inductively by open circuiting all other elements (desoldering from ground at one end), and applying small flags of copper tape to act as flux paddles.

Measurement of coupling coefficients. For first-neighbor coupling a high-pass section of two meshes with a shared leg (Fig. 3A) was constructed on the outer surface of an appropriately sized cylinder, to mimic the geometry, trace widths, and dimensions of the actual bird cage. One mesh was chosen (arbitrarily) as the reference, and resonating capacitors were applied to it, while its partner remained open circuited. The resonant frequency was measured by inductive pick at weak coupling, with an estimated uncertainty of ± 3 kHz. The reference mesh was then open circuited so that its partner could be tuned to coincidence, within the precision of the measurement, either capacitively (if it was too high) or inductively (if too low). Inductive tuning was accomplished with patches of copper tape applied to distal corners of the mesh. With the reference mesh reactivated, the symmetric and antisymmetric mode frequencies of the complete high-pass section were measured. The coupling coefficients were calculated using Eq. [13] above, which permits two determinations—one for each mode—which were averaged to give the final reported value.

The method for remote-neighbor coefficients was similar to that above except that the circuit configuration of Fig. 2B was used, and the frequencies of the individual meshes were not trimmed to coincidence; but Eq. [14] was used to extract the coupling coefficient from the uncorrected meshes.

Procedures identical to those described above were used for the shielded-bird-cage experiments, except that all measurements were performed with the model mesh circuit inside the shield.

For the TEM resonator, the appropriate pairs of resonant elements were installed inside the shielded can; the coupling geometry was that of Fig. 3C. The resonators were trimmed with flux paddles; and although no extraordinary care was taken to achieve coincidence, the maximum spread, δ, was about 0.5 MHz, but about an average resonant frequency of 147.2 MHz. No mistuning correction was applied, and the couplings were extracted from the relation $|\xi| = |\omega_+ - \omega_-|/\omega_0$.

Calculations. Frequency spectra of various resonators were calculated from Eq. [6] or [10], as appropriate, using the experimentally determined coupling coefficients and single-mesh frequencies. Calculations were performed on Mac-

TABLE 2
Comparison of Calculated and Observed Resonant Frequencies of Shielded Bird-Cage Resonators, Together with Observed Coupling Coefficients and Isolated Mesh Frequencies Used in the Calculations[a]

16-mesh low-pass bird cage	48.259 MHz[b]							
Observed	24.40	37.12	43.41	47.12	49.50	51.12	52.20	52.57
Calculated[c]	22.28	36.65	44.27	48.26	50.43	51.62	52.22	52.41
Calculated[d]	23.34	36.65	43.35	47.22	49.81	51.62	52.73	53.11
Coupling	−0.348	−0.0218						
8-mesh low-pass bird cage	42.12 MHz[b]							
Observed	30.81	42.25	46.21	47.16				
Calculated	31.00	42.12	45.55	46.37				
Coupling	−0.325							

[a] Calculated and observed frequencies are tabulated by mode number, starting from principle mode; coupling coefficients are tabulated in the order first neighbor, second neighbor, etc.
[b] Isolated single-mesh frequency.
[c] Calculated with nearest-neighbor coupling only.
[d] Calculated with nearest- and second-neighbor couplings.

intosh computers running the Matlab (Mathworks) or Mathcad (Mathsoft) packages.

RESULTS AND DISCUSSION

Table 1 shows the results for bird-cage resonators in free space and for the TEM resonator; Table 2 gives results for the shielded bird cage. The measured and calculated frequencies are tabulated along with the experimentally determined coupling coefficients and single-mesh resonant frequencies, which were used in the calculations. To assess the relative importance of near- and remote-neighbor interactions, some calculations with only near-neighbor interactions (ξ_{12} only) are also shown. The agreement of our predictions and measurements indicates that the measured couplings are of good accuracy.

It is in principle true that the magnetic coupling coefficients could be calculated from *a priori* considerations (*6, 17, 18*); but we have preferred to measure them, since simple inductance calculations are quite sensitive (*19*) to assumptions about the geometry of the conductors, and, furthermore, the accuracy of even very sophisticated calculations (*20, 21*), although impressive, has not been shown to equal that of careful measurements. In this regard, it is worth noting that the resonant frequencies of planar loops fabricated from ribbon conductors (e.g., copper tape) depend strongly upon the width of the conductor: a rectangular surface coil (of aperture 6.5 by 3.7 in., resonated with a pair of 96 pF chip capacitors) can be shifted from 40 to 38.5 MHz by simply reducing the copper width from 0.75 to 0.375 in.

While this shift of 4% might be considered small, it is outside the desired range of accuracy if bird-cage resonators are be fabricated by dead reckoning—since the main practical use of our theory is to reduce the labor of cut and try on the part of the design engineer, which is achieved only if accurate predictions, within the perturbation limit (see below), can be made from one, or at most two, measurements of coupling. Our hope has therefore been that knowledge of the near-neighbor coupling alone would enable prediction of the principal-mode frequency to an accuracy of 2%, which we take to be the maximum tolerable deviation from which a bird cage can be trimmed without the need for changing all the capacitors. This figure of 2%, while seemingly conservative, is based on a rather generous estimate of the amount of reactance which can be added to a single mesh of a bird cage, without distorting the sinusoidal current distribution of the principal mode. The reasoning is as follows: earlier perturbation calculations (*3, 16*) show that the relative frequency shift for the principal mode, $\Delta\omega/\omega$, is given by $\Delta C/(NC)$, where C is the nominal mesh capacitance, ΔC is the perturbation of capacitance applied at a single mesh, and N is the number of meshes. Since theoretical and practical study suggest that 10% is the maximum perturbation of reactance that may be applied to a single mesh without distortion, then 1.3% might be expected to be the maximum range over which the frequency could be adjusted with a single trimmer in a bird cage of 8 meshes. Applying equal trimming capacitance to 2 meshes spaced by an azimuth of π will double the range, with a relatively smaller penalty in broken symmetry. While this leads to nominal trimming ranges of 2.6% for 8 meshes, and 1.3% for 16, experience again suggests that these numbers can be stretched to 3 and 2%, respectively. Since the number of meshes in a practical bird cage rarely exceeds 16, we therefore suggest that the principal mode should be placed to within 2% of its requisite value, from which point it may be trimmed.

Our results show that this accuracy is attainable for the 8-mesh bird cage, with or without shielding, with knowledge of the near-neighbor coupling alone. However, for the 16-mesh bird cage, near-neighbor calculation gives mixed results, even without shielding, and we have found that larger resonators seem to require second-neighbor interactions for accurate predictions. For shielded bird cages of the dimensions and frequencies of the present work, the first- and second-neighbor couplings suffice. Whether this will hold for still larger resonators and/or higher frequencies remains to be seen.

The same questions of greater size and higher frequency arise for the TEM resonator in a somewhat different context. Since the structure is intuitively a low-impedance (or high-current) device, with an intrinsic shield which tends to short out electric fields, we have modeled the couplings as purely magnetic. Explicit inclusion of electric-coupling terms would involve extra terms in the numerator of [10], analogous to those which occur for the low-pass bird cage (cf. Eq. [6]), and which are due to the fact that the shunt capacitance of the rungs is a shared, or mutual, capacitance between meshes. Nonetheless, in the theory of microwave filters, the reactive coupling between resonant elements may be classified as purely inductive or capacitive. Matthei *et al.* (*22*) define a reactance-slope parameter which is used to compute coupling coefficients between elements of comb-line filters, in which all components are essentially distributed, as opposed to lumped. The important factor is then not whether a capacitive element is present (say in series with an inductor), but whether the net coupling is inductive or capacitive. Inasmuch as similar principles can be shown to apply to the bird-cage and TEM resonators, the present analysis should prove applicable beyond the quasistatic limit, and at frequencies of 1 GHz and above.

ACKNOWLEDGMENTS

The author thanks Dr. Frank Huang for supplying the resonator shields, and for assisting with some of the measurements. D.J. T. Vaughan provided helpful comments and encouragement. This work was supported by General Electric Medical Systems.

REFERENCES

1. C. E. Hayes, W. A. Edelstein, J. F. Schenck, O. M. Mueller, and M. Eash, *J. Magn. Reson.* **63,** 622 (1985).

2. P. Joseph and D. Lu, *IEEE Trans. Med. Imaging* **8,** 286 (1989).

3. J. Tropp, *J. Magn. Reson.* **82,** 51 (1989).

4. J. Tropp, Abstracts of the Society of Magnetic Resonance in Medicine, 11th Annual Meeting, p. 247, 1992.

5. M. Harpen, *Med. Phys.* **17,** 686 (1990).

6. R. Pascone, T. Vullo, J. Farrelly, and P. Cahill, *Magn. Reson. Imaging* **10,** 401 (1992).

7. P. K. H. Röschmann, United States Patent 4,746,866.

8. J. T. Vaughan, H. P. Hetherington, J. O. Otu, J. W. Pan, and G. M. Pohost, *Magn. Reson. Med.* **32,** 206 (1994).

9. H. Wen, A. S. Chesnick, and R. S. Balaban, *Magn. Reson. Med.* **32,** 492 (1994).

10. G. Matthei, L. Young, and E. M. T. Jones, ''Microwave Filters, Impedance-Matching Networks, and Coupling Structures,'' p. 214, Artech House, Dedham, 1980.

11. L. Brillouin, ''Wave Propagation in Periodic Structures,'' Chaps. 1–3, Dover, New York, 1953.

12. R. Beringer, *in* ''Principles of Microwave Circuits'' (C. G. Montgomery, R. H. Dicke, and E. M. Purcell, Eds.), Chap. 7, McGraw–Hill, New York, 1948.

13. C. A. Desoer and E. S. Kuh, ''Basic Circuit Theory,'' Chap. 10, McGraw–Hill, New York, 1969.

14. J. Tropp, Abstracts of the Society of Magnetic Resonance in Medicine, 12th Annual Meeting, p. 1347, 1993.

15. P. K. H. Röschmann, Abstracts of the Society of Magnetic Resonance and ESMRMB, p. 1000, 1995.

16. J. Tropp, *J. Magn. Reson.* **95,** 235 (1991).

17. M. C. Leifer, Abstracts of the International Society of Magnetic Resonance in Medicine, 4th Annual Meeting, p. 1420, 1996.

18. R. Srinivasan and H. Liu, Abstracts of the International Society of Magnetic Resonance in Medicine, 4th Annual Meeting, p. 1425, 1996.

19. L. D. Landau, and E. M. Lifschitz, ''Electrodynamics of Continuous Media,'' Chap. IV, Pergamon, New York, 1960.

20. H. Ochi, E. Yamamoto, K. Sawaya, and S. Adachi, Abstracts of the Society of Magnetic Resonance in Medicine, p. 1356, 1993.

21. S. M. Wright and J. R. Porter, Abstracts of the Society of Magnetic Resonance, p. 1131, 1994.

22. G. Matthei, L. Young, and E. M. T. Jones, ''Microwave Filters, Impedance-Matching Networks, and Coupling Structures,'' pp. 214–216, 432, 508, Artech House, Dedham, 1980.